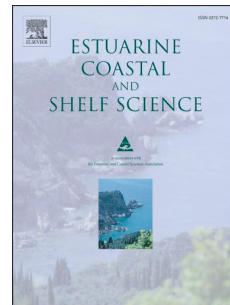


# Accepted Manuscript

Fluxes and the mass balance of mercury in Augusta Bay (Sicily, southern Italy)

Daniela Salvagio Manta, Maria Bonsignore, Elvira Oliveri, Marco Barra, Giorgio Tranchida, Luigi Giaramita, Salvatore Mazzola, Mario Sprovieri



PII: S0272-7714(16)30267-0

DOI: [10.1016/j.ecss.2016.08.013](https://doi.org/10.1016/j.ecss.2016.08.013)

Reference: YECSS 5203

To appear in: *Estuarine, Coastal and Shelf Science*

Received Date: 17 June 2015

Revised Date: 1 July 2016

Accepted Date: 12 August 2016

Please cite this article as: Manta, D.S., Bonsignore, M., Oliveri, E., Barra, M., Tranchida, G., Giaramita, L., Mazzola, S., Sprovieri, M., Fluxes and the mass balance of mercury in Augusta Bay (Sicily, southern Italy), *Estuarine, Coastal and Shelf Science* (2016), doi: 10.1016/j.ecss.2016.08.013.

This is a PDF file of an unedited manuscript that has been accepted for publication. As a service to our customers we are providing this early version of the manuscript. The manuscript will undergo copyediting, typesetting, and review of the resulting proof before it is published in its final form. Please note that during the production process errors may be discovered which could affect the content, and all legal disclaimers that apply to the journal pertain.

# Fluxes and the mass balance of mercury in Augusta Bay (Sicily, southern Italy)

Daniela Salvagio Manta<sup>a</sup>, Maria Bonsignore<sup>a</sup>, Elvira Oliveri<sup>a</sup>, Marco Barra<sup>b</sup>, Giorgio Tranchida<sup>a</sup>, Luigi Giaramita<sup>a</sup>, Salvatore Mazzola<sup>a</sup>, Mario Sprovieri<sup>a,\*</sup>

*\*(Corresponding author)*

Email address: mario.sprovieri@cnr.it

<sup>a</sup> Institute for Coastal and Marine Environment (IAMC) – CNR, Via del Mare, 3, 91021 Capo Granitola, Campobello di Mazara (TP), Italy, Tel.: +39 0924 40600

<sup>b</sup> Institute for Coastal and Marine Environment (IAMC) – CNR, Calata Porta di Massa, 80100 Naples, Italy, Tel.: +39 06 49931

## Abstract

The flux ( $\Phi$ ) of mercury (Hg) at the sediment-seawater interface was investigated in Augusta Bay (southern Italy) where uncontrolled industrial discharge from one of the most important chlor-alkali plant in Europe has caused significant negative effects on the environment. Hg fluxes were measured by the deployment of in-situ benthic chamber. The obtained value of  $1.3 \text{ kmol y}^{-1}$  clearly emphasizes the role of the sediments as source of Hg for the overlying water column. Moreover, Hg concentrations in the outflowing bottom waters were measured to estimate the export of this pollutant from Augusta Bay to the open sea. The calculated value of  $0.54 \text{ kmol y}^{-1}$ , corresponding to  $\sim 4\%$  of the anthropogenic input of Hg from coastal point/diffuse sources to the Mediterranean Sea ( $12.5 \text{ kmol y}^{-1}$ ; Rajar et al. 2007; UNEP-MAP 2001), assigns this area a crucial role in the Hg inventory of the entire Mediterranean basin. Finally, a consistent and robust mass balance for Hg in Augusta Bay was provided by combining the obtained data with Hg fluxes at seawater-atmosphere interface.

29 Keywords: mercury pollution, benthic fluxes, mass balance, Mediterranean Sea.

ACCEPTED MANUSCRIPT

## 30 **1. Introduction**

31 The need to monitor mercury in coastal marine environments is an issue of great concern, especially  
32 where the anthropogenic impact is significant. Coastal areas play a key role in the global cycle of  
33 this element (Mason et al., 1994), not only as a natural sink for terrestrially-derived Hg (Whalin et  
34 al., 2007), but also as a potential source of methylmercury in the ocean (Mason and Benoit, 2003).  
35 Despite the crucial importance of the coastal and shelf areas in the Hg biogeochemical cycle, few  
36 papers have focused on the role played by these regions as pollutant sources for the open sea,  
37 minimizing the role of Hg outflows in performing oceanic-scale mass balance (e.g., Cossa and  
38 Coquery, 2004; Rajar et al., 2007).

39 Augusta Bay, situated on the eastern Sicily (Southern Italy), is one of the most polluted area in the  
40 Mediterranean Sea, because of uncontrolled discharges (since 1950s) from petrochemical plants. In  
41 particular, the southernmost part of Augusta Bay hosted, from 1958 to 2005, an important mercury-  
42 cell chlor-alkali plant (Le Donne and Ciafani, 2008) which discharged without treatments in the  
43 bay, until restrictions were imposed by Italian law in the late 1970s (Bellucci et al., 2012).  
44 Documented effects of this indiscriminate discharges include: extremely high Hg concentrations in  
45 the bottom sediment (up to  $770 \text{ mg kg}^{-1}$ ) (ICRAM, 2008; Environ, 2008; Sprovieri et al., 2011),  
46 significant Hg evasion fluxes to atmosphere ( $\sim 10 \text{ g d}^{-1}$ ) (Bagnato et al., 2013) and a potential risk  
47 associated with local fish consumption (Ausili et al., 2008; Bonsignore et al., 2013). Furthermore,  
48 Bonsignore et al. (2015) measured Hg isotopes to trace transfer mechanisms of this toxic element  
49 from sediment to the fish compartment and eventually to the resident population in Augusta area,  
50 for which alarming increases in congenital malformations, abortions and mortality rates were  
51 recorded (Madeddu et al., 2003). Recently, Sprovieri et al. (2011) used indirect calculations to  
52 implement a Hg mass balance for the polluted Augusta Bay and estimated an outflow of  $\sim 0.16$   
53  $\text{Kmol y}^{-1}$  to the open sea, which corresponds to  $\sim 1\%$  of the Hg anthropogenic input to

54 Mediterranean sea from point and diffuse sources ( $12.5 \text{ Kmol y}^{-1}$ ; Rajar et al., 2007). This result  
55 emphasizes the role played by Augusta Bay as source of mercury at Mediterranean scale.  
56 Here, we present a revised and more quantitatively robust mass balance of Hg in Augusta Bay  
57 based on unprecedented information obtained by benthic chamber experiments, measurements of  
58 Hg in outflowing seawater and evasional fluxes to atmosphere (Bagnato et al., 2013). The study  
59 offers the valuable opportunity to provide a comprehensive vision of the geochemical cycle of Hg  
60 in Augusta Bay, with particular attention paid to the benthic fluxes. It also explores the role played  
61 by Augusta bay as potential Hg point source for the Mediterranean sea. In fact, owing to its  
62 geographical location, the outflowing shelfwater is immediately intercepted by the surface Atlantic  
63 Ionian Stream (AIS) and mixed with the main gyres of the eastern Mediterranean Sea, thus  
64 representing a risk in terms of large-scale marine system.

65

## 66 **2. Study area**

67 Augusta Bay is a natural semi-enclosed marine area of  $\sim 23.5 \text{ km}^2$ , located in Eastern Sicily (Ionian  
68 Sea, southern Italy), delimited in the northern sector by the town of Augusta and closed to South  
69 and East by artificial dams built in the early '60s (Fig. 1). It hosts one of the most important harbour  
70 of the Mediterranean Sea characterized by an intensive ship traffic. Two main mouths allow  
71 connection with the open sea: Scirocco (300 m wide and 13 m deep) and Levante inlets (400 m  
72 wide and 40 m deep). The exchanges with open sea are mainly driven by tidal fluctuations and,  
73 consequently correlated with the entry/exit of tidal flows and relative amplitudes. The input water at  
74 Levante mouth is characterized by a mean speed of  $18 \text{ cm s}^{-1}$  (depth= 0-5 m) at the surface and  $7$   
75  $\text{cm s}^{-1}$  at the bottom. (depth= 30-40 m). The input water circulation flows northward, parallel to the  
76 dam, while, the output current flows in opposite directions, with speeds of  $5\text{-}6 \text{ cm s}^{-1}$  (depth= 5-30  
77 m) The Scirocco mouth is mainly affected by outflowing water, which goes parallel to the coastline  
78 with moderate speeds ( $5\text{-}6 \text{ cm s}^{-1}$ ). Finally, the northern part of the bay is scarcely affected by active

79 currents (ICRAM, 2008; Sprovieri et al., 2011). Recent bathymetric surveys carried out by Budillon  
80 et al. (2008), showed a very narrow shelf develops down to 100–130 m with a mean gradient of  
81 about 1.0° and a steep slope characterized by a dense net of canyons dropping to the deep end of the  
82 Ionian basin (Fig. 1). As consequence of the industrial development, which has affected the area  
83 since 1960s, a wide range of pollutants has been introduced into Augusta Bay. In particular, high  
84 levels of Hg contamination resulted by the activities of the chlor-alkali plant, which discharged  
85 without treatments until the 1970s, when a demercurization plant and waste treatments became  
86 operative (Bellucci et al., 2011). Owing to the high state of environmental degradation, this area was  
87 included in 2002 in the National Remediation Plan by the Italian Environmental Ministry.

88

### 89 **3. Materials and sampling strategy**

90 The sampling strategy included the collection of seawater and sediment, as well as the placement of  
91 a benthic chamber at the bottom of the bay to estimate the Hg fluxes at the sediment-seawater  
92 interface (Fig. 1, Tab. 1). In May 2011, seawater samples were collected from the whole study-area  
93 (Fig. 1a), while sediment sampling stations (Fig. 1b) were selected in order to cover the range of Hg  
94 concentration previously reported from other studies (ICRAM, 2008; Environ, 2008; Sprovieri et  
95 al., 2011). Hg distribution obtained from the analysis of these samples drove the benthic chamber  
96 deployment performed in September 2011 and June 2012 (Fig. 1c), in order to measure fluxes from  
97 sediments characterized by different Hg pollution levels. In June 2012, also seawater and sediment  
98 were sampled in the same stations where benthic chamber experiments were performed (Fig. 1 a, b,  
99 c). Finally, in February 2012, seawater samples were collected outside the bay in order to  
100 investigate the export of Hg to open sea (Fig. 1a).

101

#### 102 **3.1 Seawater collection**

103 Seawaters were collected from 18 stations inside and 4 outside the bay, at three different depths  
104 (surface, mid-water and bottom) with a Niskin bottle rosette or a single Niskin bottle transported by

105 a scuba diver (Fig. 1a; Tab. 1). All of the samples were preserved in bottles, previously cleaned  
106 with HNO<sub>3</sub>/HCl (10%) and rinsed with Milli-Q water (18.2 MΩ cm<sup>-1</sup>). Samples were stored at -  
107 20°C until the analyses (Horvat et al., 2003). Measurements of temperature and salinity along the  
108 water column were obtained by multiparametric probe (CTD SBE 9plus).

109

### 110 **3.2 Sediment sampling**

111 Sediments were collected using a box-corer or a Plexiglas tube (length=30 cm; diameter=6 cm),  
112 manually inserted into the bottom sediment by a scuba diver (Tab. 1; Fig. 1b) and immediately  
113 stored at -20 °C until the analyses.

114

### 115 **3.3 Benthic chamber**

116 To calculate the Hg fluxes at the sediment-seawater interface, a benthic chamber was designed and  
117 assembled at the IAMC-CNR-Capo Granitola, where the base model proposed by Covelli et al.  
118 (1999, 2008) was modified. Briefly, a Plexiglas box-shape chamber (50x50x30 cm), open at the  
119 bottom side, was internally equipped with a stirring mechanism. This consisted of a rolling bar (30  
120 cm long; 5 rpm speed) moved by an electromotor (12 V) located on the top of the chamber. A  
121 plastic skirt fitted outside the chamber controls its penetration into the sediment to a depth of 7.5  
122 cm. Seawater from the benthic chamber was periodically sampled at discrete, consecutive temporal  
123 intervals (t=0, t= 1, t=4, t=6, t=10 and t=12 h) with a syringe inserted into a cap with a rubber  
124 pierceable septum. It was immediately transferred into acid-pre-cleaned vials and stored at T= -  
125 20°C until analyses.

126

## 127 **4. Analytical methods**

128 Analyses were performed at Geochemical Laboratory of IAMC-CNR - Capo Granitola. In order to  
129 minimize contamination, acid-cleaned laboratory materials and ultrapure grade reagents were used  
130 during sample preparation and analyses.

131

132 **4.1 Seawater**

133 Total (THg) and dissolved Hg (DHg) in the seawater were determined using a direct mercury  
134 analyzer (Milestone\_DMA-80) (US-EPA 7473), after oxidation with a bromine monochloride  
135 (BrCl) fresh solution (0.5 mL/100 mL sample) (US-EPA 1631). The DHg was determined after  
136 sample filtration (0.45  $\mu\text{m}$ ), in seawater samples collected from the benthic chamber and outside the  
137 bay. Blank and duplicate samples (about 20% of the of samples) were analyzed to assess detection  
138 limit (d.l.= 1.9 ng L<sup>-1</sup>; 3 $\sigma$  of the reagent blank), and reproducibility (better than 10%) of the method.  
139 Accuracy was estimated by spiked samples analysis being the certificated value of the available  
140 Reference Standard Material (BCR-579 Coastal Seawater) 1-2 orders of magnitude lower than  
141 investigated analytical range. Obtained recoveries resulted to be between 85 and 110%.

142

143 **4.2 Sediment**

144 Once defrosted, extruded from the liner, sediment cores were sectioned at 1-3 cm intervals with a  
145 stainless steel band saw. About 3.5 g of wet sediment were picked from each slide for the grain size  
146 analyses, performed with a laser granulometer (Horiba Partica LA-950V2) after treatment with  
147 H<sub>2</sub>O<sub>2</sub> (2:8) and Milli-Q water to remove organic material and cemented salts (Romano and  
148 Gabellini, 2001). The remaining sediment were dried at 35°C and powdered using an agata mortar.  
149 About 10 mg of dry sediment were loaded into specific nickel boats and analyzed by DMA-80 for  
150 Hg analysis (US-EPA 7473). A Reference Standard Material (PACS-2 Marine sediment, NRCC)  
151 was analyzed to assess accuracy (estimated to be ~7%) and precision (routinely better than 6%;  
152 RSD%, n= 3). Finally, duplicate samples (about 20% of the total samples) were analyzed to  
153 estimate the reproducibility (better than 7%). Total organic-carbon (TOC) was determined in bulk  
154 sediment by a Thermo Electron Flash EA 1112 after elimination of all the carbonate (with HCl 1M  
155 for 24 h at T<sub>ambient</sub> and drying at 60°C) (Nieuwenhuize et al., 1994).

156

## 157 **5. Results**

### 158 **5.1 Seawater**

159 Total and dissolved mercury concentrations measured in the seawater sampled within and outside  
160 Augusta Bay are reported in Table 2. The [THg] in the internal seawater vary widely from <1.90  
161 (<d.l.) to 129 ngL<sup>-1</sup> (Tab. 2), with an evident north-south increasing trend (Fig. 2).

162 The highest [THg] occurred in south-western area (S11-S25), ranging between 3.3 and 129 ngL<sup>-1</sup> in  
163 the 10-20m depth interval, between 2.27 and 127 ngL<sup>-1</sup> in the deep waters (<10m from bottom) and  
164 from <1.90 to 26.3 ngL<sup>-1</sup> in the shallow waters (>20m from bottom) (Fig. 2).

165 It is noteworthy that extremely high levels of THg were measured in S23, at the bottom ([THg]=  
166 57.8 ngL<sup>-1</sup>), and in S17, at middle and deep depths ([THg]= 129 and 127 ngL<sup>-1</sup> respectively) (Tab.  
167 2). Lower concentrations (average= 12.0±7.00 ngL<sup>-1</sup>) were found in the northern stations (S1-10)  
168 (Tab. 2). Furthermore, an increasing trend of [THg] with depth was highlighted along the seawater  
169 column, where, systematically, the surface waters show the lowest THg content (average=  
170 11.1±8.49 ngL<sup>-1</sup>), the deep waters have the highest one (average= 25.5±29.3 ngL<sup>-1</sup>) and the middle  
171 waters have intermediate THg levels (average= 20.1±29.1 ngL<sup>-1</sup>). The [THg] and [DHg] measured  
172 in seawater samples outside the bay (S26-29) varied between 2.62 and 11.9 ngL<sup>-1</sup> and between <d.l.  
173 and 5.55 ngL<sup>-1</sup>, respectively. Once again, an increasing trend of [THg] with depth was measured. In  
174 particular, the highest values (THg= 11.0 and 11.9 ngL<sup>-1</sup>; DHg= 5.55 ngL<sup>-1</sup>) were measured in the  
175 bottom seawaters (Tab. 2). The range of temperature measured inside the bay is relatively wide  
176 (from 16.6 to 20.4°C), with warmer surface water (T range= 19.0-20.4°C) and colder deep water (T  
177 range= 16.6-20.2°C). The low temperatures observed in the eastern part of the bay (S25, S13) are  
178 due to the input of relatively colder water from the open sea, with measured values ranging from  
179 13.9 to 15.2 °C (Tab. 2). Salinity ranges from 36.7 to 39.0 *psu* inside and between 37.9 and 38.9 *psu*  
180 outside the bay. The lower values recorded inside the bay are probably due to inputs of freshwater  
181 or sewage from land (Tab. 2).

182

183 **5.2 Sediment**

184 Grain size, TOC and [Hg] measured in the sediment are reported in Figure 3 (a, b, c, respectively)  
185 and Appendix I.

186 Almost all of the analyzed samples consist of silt (more than 50%) and clay (32-45%), whereas the  
187 sandy fraction represents a small percentage (~10%). Only the S19 core is sandy (~70%) and  
188 contains small amounts of silt (~17%) and clay (~13%). The calculated sorting parameter (ranging  
189 from 4.8 to 12.2  $\mu\text{m}$ ) is indicative of a low energy environment, where the slow current circulation  
190 affects the poor size selection of the sediment (Fig. 3a).

191 All samples show high TOC (from 1.58 to 4.26%), thus suggesting relatively high  
192 burial/preservation of organic matter in the sediment. In the southern S21, the values range widely  
193 from 1.58 to 3.45% (average=  $2.32\pm 0.50\%$ ) with an irregular distribution along the core,  
194 characterized by an evident peak (3.45%) at 14-16 cm. In the S15 core, the TOC-depth profile is  
195 quite constant except for two peaks at 2-4 cm (2.85%) and 20-22 cm (4.26%) (average=  
196  $2.38\pm 0.68\%$ ). The lowest mean value ( $2.27\pm 0.11\%$ ) was measured in the northern station (S7),  
197 where TOC show a steady trend with depth (Fig. 3b).

198 The measured [THg] varies widely (from 1.77 to 55.3  $\text{mgKg}^{-1}$ ) (Fig. 3b). The highest values were  
199 found in the southern stations, specifically in the intermediate part (6-21 cm) of the core S14, with  
200 [THg] ranging between 20.8 and 39.5  $\text{mgKg}^{-1}$ , and along the core S21, where the values vary  
201 between 19.0 and 55.3  $\text{mgKg}^{-1}$ , in the interval from 4 to 30 cm). Moreover, the concentration-depth  
202 profiles in cores S14 and S21 are characterized by a marked peak between 12 and 16 cm, whereas  
203 nearly steady trends were measured in the remaining cores. The lowest values were found in the  
204 northern stations, with average concentrations of  $6.33\pm 0.91 \text{ mgKg}^{-1}$  in S7,  $6.15\pm 1.54 \text{ mgKg}^{-1}$  in S8;  
205 and in the sandy S19 core (average=  $7.81\pm 1.66 \text{ mgKg}^{-1}$ ) collected from the southern area (average=  
206  $7.81\pm 1.66 \text{ mgKg}^{-1}$ ). Finally, intermediate values were measured in S15 (average=  $12.5\pm 2.66 \text{ mgKg}^{-1}$ )  
207 and S16 (average=  $16.2\pm 1.66 \text{ mgKg}^{-1}$ ) (Fig. 3c).

208

209 **5.3 Benthic fluxes**

210 The DHg content in the seawater at the sediment-seawater interface increased with time at all  
 211 stations (Appendix II, Fig. 4). Specifically, the increasing trend was constant for the entire  
 212 incubation period (0-10/12h) in chambers 18 and 21, while in the other stations the DHg content  
 213 exhibited a major increase in the first hour (0-1h), but was almost constant during the time interval  
 214 that followed (1-10/12h) (Fig. 4). The mercury fluxes across the sediment-seawater interface were  
 215 calculated on the basis of the best fit curve “concentration vs time”, according to the following  
 216 equation (Santschi et al., 1990) (1):

$$217 \quad \phi Hg = \left( \frac{\delta C}{\delta t} \times \frac{V}{A} \right) \quad (1)$$

218 where:

219  $\delta C/\delta t$  = variation of the Hg concentration over time ( $\text{ng L}^{-1} \text{h}^{-1}$ ).220  $V$  = volume of the benthic chamber (57.5 L).221  $A$  = cover area of the sea-bottom ( $0.25 \text{ m}^2$ ).

222

223 Finally, the obtained results were normalized to 24h. The mercury fluxes per day calculated in the  
 224 northern area were very comparable in the neighboring S7 and S9 ( $22.7$  and  $22.6 \mu\text{g m}^{-2} \text{d}^{-1}$ ,  
 225 respectively) (Fig. 4). Conversely, in the southern area, significant differences among the stations  
 226 were observed. In particular, S15 and S22 had the highest values ( $92$  and  $56 \mu\text{g m}^{-2} \text{d}^{-1}$ ,  
 227 respectively), while relatively low flux ( $8.7 \mu\text{g m}^{-2} \text{d}^{-1}$ ) were estimated for S18, despite the closeness  
 228 to S21, where a higher flux of  $20.5 \mu\text{g m}^{-2} \text{d}^{-1}$  was recorded (Fig. 4). The calculated fluxes were  
 229 extended to a yearly estimation and then over the entire area using the territorial distribution model  
 230 proposed by Aurenhammer (1991) (Voronoi Polygons method). The estimated fluxes amounted to  
 231  $1.1 \text{ kmol y}^{-1}$  in September 2011 ( $0.22 \text{ t y}^{-1}$ ) and  $1.4 \text{ kmol y}^{-1}$  ( $0.29 \text{ t y}^{-1}$ ) in June 2012.

232

233 **6. Discussion**

234 The [Hg] measured in Augusta Bay sediment are extremely elevated (Fig. 3c), being 1-2 orders of  
235 magnitude higher than the Mediterranean background values (0.04-0.17 mgKg<sup>-1</sup>) (e.g., Donazzolo  
236 et al., 1981; Ogrinc et al., 2007). They are also comparable with the values (4.06 and 79.0 mg Kg<sup>-1</sup>)  
237 reported for sediment of other coastal areas affected by relevant industrial or mining activities (e.g.,  
238 Baldi and Bergagli, 1984; Covelli et al., 2001, 2008, 2011; Emili et al., 2012). The higher  
239 concentrations, measured in the southern stations, can be attributable to industrial input (~2.1 kg y<sup>-1</sup>  
240 <sup>1</sup>; value reported by the European Pollutant Emission Register) and to the proximity of the most  
241 important chemical and petrochemical plants (Syndial Priolo Gargallo, ESSO, ERG, etc.). In  
242 particular, the chlor-alkali plant, is considered to have been the main Hg source in the bay (Di  
243 Leonardo et al., 2007; ICRAM, 2008; Sprovieri et al. 2011; Bellucci et al., 2012), with an average  
244 discharge of about 260 kg y<sup>-1</sup> of Hg estimated between early-1960 and late-1970 (Colombo et al.,  
245 2005). However, in Augusta Bay, effects of re-suspension due to the intensive ship traffic,  
246 combined with relevant dredging activities occurred since 1960s, make the historical reconstruction  
247 of industrial contaminant inputs very difficult to be achieved without a specific integrated approach  
248 (Cundy et al., 2003; Bellucci et al., 2012). Concentrations measured in the studied cores are in good  
249 agreement with the Hg areal distribution in surface sediment reported by Sprovieri et al. (2011),  
250 which subdivided Augusta Bay in two geographical sectors characterized by significantly different  
251 levels of contamination: i) a southern sector ([Hg] median value=23.8 mgKg<sup>-1</sup>) affected by chemical  
252 and petrochemical plants activity and ii) a northern sector ([Hg] median value= 1.1 mg Kg<sup>-1</sup>)  
253 affected by municipal waste discharge. The only exception is represented by S19 core,  
254 characterized by Hg contents lower than those found in the neighboring stations. It is probably due  
255 to its specific sandy grain-size composition (Fig. 3a) responsible for a less Hg adsorbing capacity  
256 (Ravichandran, 2004). On the other hand, a positive correlation was found between [Hg] and finer  
257 grain-size fraction for S14 (r<sup>2</sup>= 0.7) and S21 (r<sup>2</sup>= 0.5), where specifically, the highest Hg levels  
258 correspond to the highest silt-clay percentages (92 and 95%) (Fig. 3 c, a). The high TOC values

259 measured (Fig. 3, Appendix I) are compatible with the disoxic/anoxic conditions measured at the  
260 bottom basin (average  $E_h \sim -300$  mV; ICRAM, 2008; Sprovieri et al., 2011) and possibly due to the  
261 state of semi-closed environment of the basin and the low energy hydrodynamics. Noteworthy, high  
262 contents of organic matter under reducing environmental conditions promote methylation processes,  
263 mediated by microorganisms, such as sulfate reducing bacteria (SRB), at water/sediments interface  
264 (e.g., Langer et al., 2001; Lambertsson and Nilsson 2006). Thus, bottom sediments in Augusta bay  
265 represent a potential source of methylmercury (MeHg) for the ecosystem which could also partially  
266 justify the high levels of Hg found in fish caught in the bay (Bonsignore et al., 2013, 2016).

267 .A significant statistical correlation ( $r^2 = 0.71$ ) between [THg] and TOC, was found in the core S21,  
268 where peaks of Hg corresponding to the highest TOC values (Fig. 3 c, b) occur. Conversely, no  
269 positive correlation was recorded in the other cores (S7, S15). The north-south positive gradient of  
270 [Hg] in the Augusta sediment is reflected in the spatial distribution of THg in seawater, with lower  
271 values recorded in the northern area and higher ones in the south (Fig. 2). Noteworthy, an evident  
272 [THg] vertical increasing trend was observed along the water column (Fig. 2, Tab. 2), with the  
273 lowest concentrations measured in the surface layers, where the penetrating sunlight promotes the  
274 photoreduction and the subsequent volatilization of  $Hg^0$  form (Fitzgerald and Clarkson, 1991;  
275 Bagnato et., 2013), and the highest values found close to the bottom, where resuspension events and  
276 Hg release from sediment probably affect the concentration of this pollutant in the overlying water  
277 column. In the marine environment, Hg is generally bound to sediment through: ion exchange,  
278 complexing or chelation with organic and inorganic ligands, sorption with Fe/Mn oxide-hydroxides  
279 or incorporation into mineral lattice (Ramamoorthy and Massalki, 1979). However, changes in  
280 physical-chemical parameters at the sediment-seawater interface, bioturbation, dredging activities  
281 and methylation, may result in remobilization and diffusion of the Hg in the water column (Covelli  
282 et al., 1999). In this study, benthic chamber experiments provided direct measurement of Hg fluxes  
283 from the sediment to the overlying seawater. The obtained values vary widely between 8.7 and 92  
284  $\mu g m^{-2} d^{-1}$ . These differences could be attributed to variable Hg concentrations in surface sediments

285 (Appendix I), where comparable physical-chemical conditions at the seawater-sediment interface  
286 and analogue Hg speciation occurs, as well-demonstrated by Oliveri et al. (2016, *in press*). The  
287 measured benthic fluxes are higher than those estimated for other contaminated areas (5 and 10  $\mu\text{g}$   
288  $\text{m}^{-2} \text{d}^{-1}$ ) (Bothner et al., 1980; Covelli et al., 1999; Boucher et al., 2011) and comparable with values  
289 reported by Covelli et al. (2008) for the highly-contaminated Grado Lagoon (37 and 77  $\mu\text{g} \text{m}^{-2} \text{d}^{-1}$ ). ,  
290 The flux at the sediment-seawater interface estimated for the entire bay ( $1.3 \pm 0.1 \text{ kmol y}^{-1}$ ) is about  
291 two orders of magnitude higher than that of the evasion into the atmosphere ( $1.8 \times 10^{-2} \text{ kmol y}^{-1}$ )  
292 (Bagnato et al., 2013). This could imply that a relevant part of the Hg released in seawater is  
293 recycled in the biogeochemical cycle (biota uptake, adsorption by suspended particulate matter, re-  
294 deposition) and/or outflows to the open sea. This latter hypothesis is supported by the anomalous  
295 Hg concentrations measured in the seawater outside Augusta Bay (Tab. 2), which were an order of  
296 magnitude higher than the Mediterranean background values (0.2-0.4  $\text{ng L}^{-1}$ ) (Cossa et al., 1997;  
297 Horvat et al., 2003; Kotnik et al., 2007; Rajar et al., 2007). This is in agreement with the data  
298 reported by Fantozzi et al., (2012), which measured unusual Hg contents in seawater out Augusta  
299 Bay (4.8 and 18  $\text{ngL}^{-1}$ ) and argued that the water circulation in the Strait of Sicily moves polluted  
300 masses from Augusta Bay eastwards. Moreover, Sprovieri et al. (2011) speculated that the effects of  
301 the meso-scale circulation of the Ionian Sea, together with a narrow shelf and a steep slope off  
302 Augusta Bay (Budillon et al., 2008) (Fig. 1), create a high potential risk of Hg contamination of the  
303 Mediterranean basin. This evidence calls for an appropriate estimate of the possible outflow of this  
304 pollutant from Augusta Bay to the open sea. To this aim, we took in account the DHg  
305 concentrations measured in the bottom water just outside Scirocco and Levante mouths (5.6 and 3.6  
306  $\text{ng L}^{-1}$ , respectively; Tab. 2) and the associated relative outputs of seawater ( $2.34 \times 10^{13} \text{ kg y}^{-1}$ ), as  
307 reported by Sprovieri et al. (2011). Thus, the estimated Hg outflow resulted to be  $0.54 \text{ kmol y}^{-1}$ .  
308 This value corresponds to ~4% of the anthropogenic input of Hg from coastal point/diffuse sources  
309 to the Mediterranean Sea ( $12.5 \text{ kmol y}^{-1}$ ; Rajar et al. 2007; UNEP-MAP 2001), and definitively  
310 emphasizes the role played by Augusta Bay as a crucial "point source" at the basin scale.

311

312 *Mass balance of Hg in Augusta Bay*

313 A steady-state mass balance for mercury, calculated to explore the geochemical cycle of this  
 314 pollutant within the Augusta Bay, is here proposed. For this purpose, the Augusta Bay was basically  
 315 considered as an “environmental compartment” with well-defined borders and constrained  
 316 hydrodynamics. According to the basic scheme proposed by Sprovieri et al. (2011), we applied the  
 317 following equation:

318

$$319 \quad \mathbf{I+A+AD+R = O+D+V} \quad (2)$$

320 where:

321 I = total Hg influx from the surface Mediterranean seawater

322 A= input of dissolved Hg from anthropogenic activities

323 AD= atmospheric Hg deposition

324 R= Hg re-suspension/release from the sediment

325 O= Hg outflow from the basin to the open sea

326 D= amount of Hg recycled into Augusta Bay (buried in sediment and/or accumulated in the biota)

327 V= Hg evasion into the atmosphere

328

329 The total seawater Hg influx value (I) was estimated using data reported by Kotnik et al. (2007), and  
 330 corresponded to an average input of Hg from the Ionian Sea to Augusta Bay of about  $3.12 \pm 0.94 \times$   
 331  $10^{-2} \text{ kmol y}^{-1}$ . The anthropogenic Hg input into the basin (A), including discharges from wastewater  
 332 treatment facilities and industrial activities (*Erg, Syndyal, Esso*) was considered to be  $6.2 \times 10^{-2}$   
 333  $\text{kmol y}^{-1}$  (value reported by the European pollutant emission register for the year 2005). AD and V  
 334 corresponded to the values reported by Bagnato et al. (2013) ( $0.42 \times 10^{-2} \text{ kmol y}^{-1}$  and  $1.7 \pm 0.02 \times$   
 335  $10^{-2} \text{ kmol y}^{-1}$ , respectively). Finally, O and R are the values measured in this study, which  
 336 correspond to the Hg outflow from the bay to the open sea ( $0.54 \pm 0.08 \text{ kmol y}^{-1}$ ), and the Hg flux  
 337 from the sediment to the seawater ( $1.3 \pm 0.2 \text{ kmol y}^{-1}$ ), respectively. In particular, the last term  
 338 represents the final result of Hg diffusion from porewater and desorption from re-suspended of

339 organic/inorganic particles. Thus, the Hg recycled (re-deposited and/or accumulated in the biota as  
340 MeHg) into the bay (D) results to be  $0.84\pm 0.22$  kmol  $y^{-1}$ , which represents from ~45 to 75% of the  
341 total input of Hg in the Augusta Bay. while the remaining part escapes into atmosphere (1-2%) and  
342 outflows to open sea (average ~40%). This means that the Augusta Bay plays an important role in  
343 recycling and exporting of mercury into the Mediterranean Sea and represents a relevant point  
344 source for that system.

345 This study definitively states how strong interlinks between contaminants behaviour and ocean  
346 dynamics drive the specific control of point sources on widespread distribution of pollutants. In  
347 particular, this offers a good science-driven case for an appropriate conceptual approach to the  
348 Marine Strategy Framework Directive (2008/56/EC), which specifically states that it should be  
349 possible to determine how to keep the pressure of human activities within levels compatible with  
350 the preservation or restoration of a Good Environmental Status in the Mediterranean sea, from 2020  
351 onwards.

### 353 **Acknowledgements**

354 This work forms part of the IAMC-CNR/ASP project funded by the “Assessorato della Salute” of  
355 Sicily. The authors gratefully acknowledge the personnel of the Port Authority of Augusta and Dr.  
356 F. Bulfamante from IAMC-CNR (Capo Granitola) for their logistical support. The authors would  
357 also like to express sincere thanks to Vincenzo Di Stefano, Igor Bisulli, Carmelo Buscaino, Gaspare  
358 Buffa and Carlo Patti, for their efforts during the sampling.

### 360 **Figure captions:**

361 **Figure 1:** Sampling location of the seawater (a), sediment (b) and benthic chamber (c) in the  
362 Augusta Bay.

363 **Figure 2:** Map of [THg] distribution in seawaters collected during May 2011; a) 0-10m from the  
 364 bottom; b) 10-20m from the bottom; c) 20m from the bottom up to surface. Maps were created  
 365 through 3D block kriging and were themed on the “natural breaks” method.

366 **Figure 3:** Profile of TOC (a), [Hg] (b) and grain size composition (b) along the collected cores.

367 **Figure 4:** Concentration of DHg vs. time during the benthic chamber experiment.

368

## 369 References

- 370 Acquavita, A., Covelli S., Emili A., Berto D., Faganeli J., Giani M., Horvat M., Koron N., Rampazzo F.  
 371 Mercury in the sediments of the Marano and Grado Lagoon (northern Adriatic Sea): Sources,  
 372 distribution and speciation. *Estuar.Coast.Shelf.S.* (2012),13,20-31
- 373 Aurenhammer, F. Voronoi diagrams—a survey of a fundamental geometric data structure. *ACM Computing*  
 374 *Surveys* (1991), 23(3),345–405
- 375 Ausili, A., Gabellini, M., Cammarata, G., Fattorini, D., Benedetti, M., Pisanelli, B., Gorbi, S., Regoli, F.,  
 376 Ecotoxicological and human health risk in a petrochemical district of southern Italy. *Mar.Environ.Res.*  
 377 (2008),66,215–217
- 378 Bagnato, E., Sproveri, M., Barra, M., Bitetto, M., Bonsignore, M., Calabrese, S., Di Stefano, V., Oliveri, E.,  
 379 Parello, F., Mazzola, S. The sea–air exchange of mercury (Hg) in the marine boundary layer of the  
 380 Augusta basin (southern Italy): Concentrations and evasion flux. *Chemosphere* (2013),93, 2024–2032
- 381 Baldi, F., Bargagli, R. Mercury pollution in marine sediments near a chlor-alkaly plant: distribution and  
 382 avail- ability of the metal. *Sci.Tot.Environ.* (1984),39,15-26
- 383 Bellucci, L. G., Giuliani, S., Romano, S., Albertazzi, S., Mugnai, C. and Frignani M. An Integrated  
 384 Approach to the Assessment of Pollutant Delivery Chronologies to Impacted Areas: Hg in the Augusta  
 385 Bay (Italy). *Environ. Sci. Technol.* (2012), 46, 2040–2046.
- 386 Bonsignore M., Andolfi, N., Barra, M., Madeddu, M., Tisano, F., Ingallinella, V., Castorina, M., Sprovieri,  
 387 M. Assessment of mercury exposure in human populations: A status report from Augusta Bay  
 388 (southern Italy). *Environmental Research*, Special Issue: Human biomonitoring. *In Press*, Corrected  
 389 Proof, Available online 19 January 2016. DOI: 10.1016/j.envres.2016.01.016
- 390 Bonsignore M.; Tamburrino S., Oliveri E., Marchetti A., Durante C., Berni A., Quinci E., Sprovieri M.  
 391 Tracing mercury pathways in Augusta Bay (southern Italy) by total concentration and isotope  
 392 determination. *Environmental Pollution* 2015, DOI: 10.1016/j.envpol.2015.05.033
- 393 Bonsignore, M., Salvagio Manta, D., Oliveri, E., Sprovieri, M., Basilone, G., Bonanno, A., Falco, F., Traina,  
 394 A., Mazzola S. Mercury in fishes from Augusta Bay (southern Italy): Risk assessment and health  
 395 implication. *Food and Chemical Toxicology* (2013), 56,184–194
- 396 Bothner, M.H., Jahnke, R.A., Peterson, M.L., Carpenter, R. Rate of loss from contaminated estuarine  
 397 sediments. *Geochim.Cosmochim.Ac.* (1980),44,273– 285
- 398 Bouchet, S., Tessier, E., Monperrus, M., Bridou, R., Clavier, J., Thouzeau, G. and Amouroux, D.  
 399 Measurements of gaseous mercury exchanges at the sediment–water, water–atmosphere and sediment–  
 400 atmosphere interfaces of a tidal environment (Arcachon Bay, France). *J.Environ.Monit.*  
 401 (2011),13,1351
- 402 Budillon, F., Ferraro, L., Hopkins, T.S., Iorio, M., Lubritto, C., Sprovieri, M., Bellonia, A., Marzaioli, F.,  
 403 and Tonielli, R. Effects of intense anthropogenic settlement of coastal areas on seabed and  
 404 sedimentary systems: a case study from the Augusta Bay (Southern Italy), *Rendiconti online Societa*  
 405 *Geologica Italiana*, 2008, 3, 142–143
- 406 Colombo, F., Frignani, M., and Bellucci, L.. Origine storica della contaminazione dei sedimenti della Rada  
 407 di Augusta. (2005) October

- 408 Cossa D., Martin J.-M., Takayanagi K., and Sanjuan J. The distribution and cycling of mercury species in the  
409 western Mediterranean. *Deep-Sea Res. II* (1997) 44(3–4),721–740
- 410 Cossa, D., Coquery, M. The Mediterranean mercury anomaly, a geochemical or a biological issue. Handbook  
411 of Environmental Chemistry, Review Series in Chemistry (2004) The Mediterranean (Salot, a.,  
412 Editor), vol. 5,39
- 413 Covelli, S., Emili, A., Acquavita, A., Koron, N., Faganeli, J. Benthic biogeochemical cycling of mercury in  
414 two contaminated northern Adriatic coastal lagoons. *Cont.Shelf.Res.* (2011),31, 1777-1789.
- 415 Covelli, S., Faganeli, J., De Vittor, C., Predonzani, S., Acquavita, A. and Horvat, M. Benthic fluxes of  
416 mercury species in a lagoon environment (Grado Lagoon, Northern Adriatic Sea, Italy). *Appl*  
417 *Geochem.* (2008), 23,529–546
- 418 Covelli, S., Faganeli J., Horvat, M., Brambati, A. Mercury contamination of coastal sediments as the result  
419 of long-term cinnabar mining activity (Gulf of Trieste, northern Adriatic sea). *Appl.Geochem.*  
420 (2001),16,541-558
- 421 Covelli, S., Faganeli, J., Horvat M. and Brambati, A. Porewater Distribution and Benthic Flux Measurements  
422 of Mercury and Methylmercury in the Gulf of Trieste (Northern Adriatic Sea). *Estuar.Coast.Shelf.S.*  
423 (1999),48,415–428
- 424 Cundy, A. B., Croudace, I. W., Thomson, J., Lewis, J. T. Reliability of salt marshes as “geochemical  
425 recorders” of pollution input: a case study from contrasting estuaries in Southern England. *Environ.*  
426 *Sci. Technol.* (1997), 31, 1093–1101.
- 427 Di Leonardo, R., Bellanca, A., Capotondi, L., Cundy, A., Neri, R., Possible impacts of Hg and PAH  
428 contamination on benthic foraminiferal assemblages: An example from the Sicilian coast, central  
429 Mediterranean. *Science of the Total Environment* 388 (2007) 168–183
- 430 Donazzolo, R., Hieke Merlin, O., Menegazzo Vitturi, L., Orio, A.A., Pavoni, B., Perin, G. et al. Heavy metal  
431 contamination in surface sediments from the Gulf of Venice, Italy. *Mar.Pollut.Bull.* (1981),12,417-425
- 432 Emili, A., Acquavita, A., Koron, N., Covelli, S., Faganeli, J., Horvat, M., Žižiek, S., Fajon, V. Benthic flux  
433 measurements of Hg species in a northern Adriatic lagoon environment (Marano and Grado Lagoon,  
434 Italy). *Estuar.Coast.Shelf.S.* (2012),113,71-84
- 435 Environ International Team. Appendix A Sediment Investigation Activities Performed by ENVIRON  
436 Summer and Fall (2008) Augusta Bay, Sicily, Italy
- 437 EPA (Environmental Protection Agency). Method 1631, Revision E: Mercury in Water by Oxidation, Purge  
438 and Trap, and Cold Vapor Atomic Fluorescence Spectrometry (2002)
- 439 EPA (Environmental Protection Agency). Method 7473. “Mercury in solids and solutions by thermal  
440 decomposition, amalgamation, and atomic absorption spectrophotometry” (2007)
- 441 European pollutant emission register, [http://www.eper.sinanet.apat.](http://www.eper.sinanet.apat.it/site/itIT/Registro_INES/Ricerca_per_complesso_industriale/ricercaINES.html)  
442 [it/site/itIT/Registro\\_INES/Ricerca\\_per\\_complesso\\_industriale/ricercaINES.html](http://www.eper.sinanet.apat.it/site/itIT/Registro_INES/Ricerca_per_complesso_industriale/ricercaINES.html)
- 443 Fantozzi, L., Manca, G., Ammoscato, I., Pirrone, N., Sprovieri, F. The cycling and sea–air exchange of  
444 mercury in the waters of the Eastern Mediterranean during the 2010 MED-OCEANOR cruise  
445 campaign. *Sci.Total.Enviroin.* (2012),448,151–162
- 446 Fitzgerald, W. F. and Clarkson, T. W.. Mercury and monomethylmercury: present and future concerns.  
447 *Environ.Health.Perspect.* (1991),96,159–166
- 448 Horvat, M., Kotnik, J., Logar, M., Fajon, V., Zvonari C., T., Pirrone, N. Speciation of mercury in surface and  
449 deep-sea waters in the Mediterranean Sea. *Atmos.Enviroin.* (2003),37,S93eS108
- 450 ICRAM. Istituto Centrale Per La Ricerca Scientifica E Tecnologica Applicata Al Mare, Progetto preliminare  
451 di bonifica dei fondali della rada di Augusta nel sito di interesse nazionale di Priolo – Elaborazione  
452 definitiva, BoI-Pr-SI-PR-Rada di Augusta-03.22, (2008),182
- 453 Kotnik, J., Fajon, V., Gibičar, D., Logar, L., Horvat, N., Ogrinc, N., Horvat, M., Amouroux, D., Monperrus,  
454 M., Sprovieri F. and Pirrone N. Mercury speciation in surface and deep waters of the Mediterranean  
455 and Adriatic seas. *Mar.Chem.* (2007),107,13–30

- 456 L. Lambertsson and M. Nilsson, Organic material: the primary control on mercury methylation and ambient  
457 methyl mercury concentrations in Estuarine sediments, *Environ. Sci. Technol.* (2006), 40, 1822–1829
- 458 C. Langer, W. Fitzgerald, P. Visscher and G. Vandal. Biogeochemical cycling of methylmercury at Barn  
459 Island Salt Marsh, Stonington, CT, USA, *Wetlands Ecol. Manage.* (2001), 9, 295–310
- 460 Le Donne, K., Ciafani, S. Monitoraggio dell'inquinamento atmosferico da mercurio nei principali impianti  
461 cloro-soda italiani. *Ing. Ambientale* (2008), 37, 45–52
- 462 Madeddu, A., Contrino, L., Tisano, F., Sciacca S.. La peste, gli untori e l'immaginario. Atlante della  
463 mortalità per tumori e per le patologie cronico degenerative in provincia di Siracusa dal 1995. Volume  
464 II (2003)
- 465 Mason, R. P., Fitzgerald W. F., and Morel F. M. M. (MFM). The biogeochemical cycling of elemental  
466 mercury: anthropogenic influences. *Geochim. Cosmochim. Acta* (1994), 58, 3191–3198
- 467 Mason, R. P., Rolffhus, K. R., and Fitzgerald W. F. Mercury in the North Atlantic. *Mar. Chem.* (1998), 61, 37–  
468 53
- 469 Mason, R.P., Benoit, J.M.. Organomercury compounds in the environment. In: Craig, P. (Ed.),  
470 Organometallics in the Environment. *John Wiley & Sons, NY* (2003), 57–99
- 471 Nieuwenhuize, J., Maas, Y.E.M., Middelburg, J.J.. Rapid analysis of organic carbon and nitrogen in  
472 particulate materials. *Mar. Chem.*, (1994), 45, 217–224
- 473 Ogrinc, N., Kotnik, J., Fajon, V., Monperrus, M., Kocman, D., Vidimova, K., Amouroux, D., Žižek S. and  
474 Horvat, M. Distribution of mercury and methylmercury in sediments of the Mediterranean sea.  
475 *Mar. Chem.* (2007), 107, 31–48
- 476 Oliveri, E., Salvagio Manta, D., Bonsignore, M., Cappello, S., Tranchida, G. Bagnato, E. Sabatino, N.  
477 Santisi, S. Sprovieri, M. (2016) Mobility of mercury in contaminated marine sediments:  
478 biogeochemical pathways. *Marine Chemistry* (in press).
- 479 Rajar, R., Četina, M., Horvat, M. and Žagar, D. Mass balance of mercury in the Mediterranean Sea.  
480 *Mar. Chem.* (2007), 107, 89–102
- 481 Ramamoorthy, S., Massalki, A. Analysis of structure- localized mercury in Ottawa river sediments by  
482 scanning electron microscopy/energy-dispersive X-ray microanalysis technique. *Environ. Geol.*  
483 (1979), 6, 351–357
- 484 Ravichandran, M. Interactions between mercury and dissolved organic matter, a review. *Chemosphere*  
485 (2004), 55, 319–331
- 486 Romano, Gabellini. Metodologie analitiche di riferimento – Ministero dell'Ambiente e della Tutela del  
487 Territorio – Servizio Difesa Mare. Programma di monitoraggio per il controllo dell'ambiente marino-  
488 costiero (triennio 2001-2003) (2001)
- 489 Santschi, P., Hohener, P., Benoit, G. & Bucholtz-ten Brink, M. Chemical processes at the sediment–water  
490 interface. *Marine Chemistry* (1990), 30, 315–369
- 491 Sprovieri, M., Oliveri, E., Di Leonardo, R., Romano, E., Ausili, A., Gabellini, M., Barra, M., Tranchida, G.,  
492 Bellanca, A., Neri, R., Budillon, F., Saggiomo, R., Mazzola, S., Saggiomo, V. The key role played by  
493 the Augusta basin (southern Italy) in the mercury contamination of the Mediterranean sea. *J. Environ.*  
494 *Monit.* (2011), 13, 1753
- 495 UNEP-MAP, 2001. Protecting the Mediterranean from Land-based Pollution. Athens. 47 pp.
- 496 Whalin, L., Kim, E. H., Mason, R.. Factors influencing the oxidation, reduction, methylation and  
497 demethylation of mercury species in coastal waters. *Mar. Chem.* (2007), 107, 278–294

**Table 1:** Details of the sampling performed in Augusta Bay.

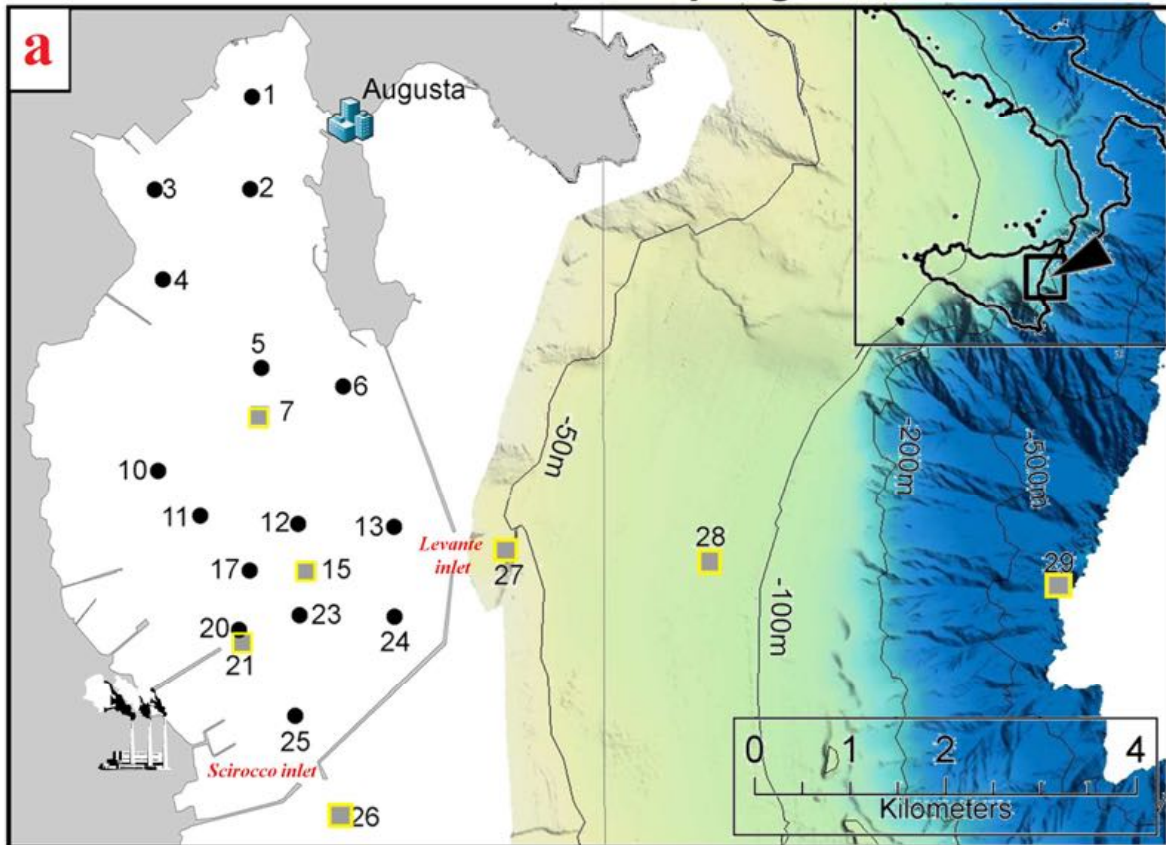
| Sampling  | Vessel               | Period                  | Station         |            | Bottom depth<br>(m) | Method of sampling |                              |           |
|---|----------------------|-------------------------|-----------------|------------|---------------------|--------------------|------------------------------|-----------|
|   |                      |                         | Lat.            | Long.      |                     |                    |                              |           |
| Seawaters   | N/O<br>G. Dallaporta | 23-<br>26/05/11         | 1               | 37°14.392N | 15°12.537E          | 14.0               | Niskin                       |           |
|   |                      |                         | 2               | 37°13.864N | 15°12.519E          | 16.0               |                              |           |
|   |                      |                         | 3               | 37°13.863N | 15°11.845E          | 11.0               |                              |           |
|   |                      |                         | 4               | 37°13.353N | 15°11.902E          | 8.00               |                              |           |
|   |                      |                         | 5               | 37°12.849N | 15°12.595E          | 20.0               |                              |           |
|   |                      |                         | 6               | 37°12.743N | 15°13.176E          | 17.0               |                              |           |
|   |                      |                         | 10              | 37°12.267N | 15°11.863E          | 22.0               |                              |           |
|   |                      |                         | 11              | 37°12.009N | 15°12.161E          | 22.0               |                              |           |
|   |                      |                         | 12              | 37°11.961N | 15°12.855E          | 27.0               |                              |           |
|   |                      |                         | 13              | 37°11.943N | 15°13.536E          | 32.0               |                              |           |
|   |                      |                         | 17              | 37°11.696N | 15°12.512E          | 24.0               |                              |           |
|   |                      |                         | 20              | 37°11.363N | 15°13.536E          | 21.0               |                              |           |
|   |                      |                         | 23              | 37°11.445N | 15°12.434E          | 22.0               |                              |           |
|   |                      |                         | 24              | 37°11.434N | 15°13.536E          | 21.0               |                              |           |
|   |                      |                         | 25              | 37°10.871N | 15°12.833E          | 16.0               |                              |           |
|   | N/O<br>Urania        | 02/02/12                | 26              | 37°10.310N | 15°13.148E          | 17.0               | Niskin                       |           |
|   |                      |                         | 27              | 37°11.807N | 15°14.328E          | 42.0               |                              |           |
|   |                      |                         | 28              | 37°11.742N | 15°15.767E          | 85.0               |                              |           |
|   |                      |                         | 29              | 37°11.604N | 15°18.240E          | 679                |                              |           |
|   | M/N<br>L. Sanzo      | 23-<br>26/06/12         | 7               | 37°12.578N | 15°12.583E          | 22.8               | Single Niskin bottle         |           |
|   |                      |                         | 15              | 37°11.697N | 15°12.917E          | 27.8               |                              |           |
|   |                      |                         | 21              | 37°11.288N | 15°12.459E          | 22.8               |                              |           |
|   | Sediments            | N/O<br>G.<br>Dallaporta | 23-<br>26/05/11 | 8          | 37°12.618N          | 15°12.473E         | 22.0                         | Box-corer |
|   |                      |                         |                 | 14         | 37°11.745N          | 15°12.985E         | 28.0                         |           |
|   |                      |                         |                 | 16         | 37°11.818N          | 15°12.540E         | 27.0                         |           |
| 19  |                      |                         |                 | 37°11.399N | 15°12.375E          | 21.0               |                              |           |
| M/N<br>L. Sanzo                                   |                      | 23-<br>26/06/12         | 7               | 37°12.578N | 15°12.583E          | 22.8               | Manual corer                 |           |
|   |                      |                         | 15              | 37°11.697N | 15°12.917E          | 27.8               |                              |           |
|   |                      |                         | 21              | 37°11.288N | 15°12.459E          | 22.8               |                              |           |
| Seawater at<br>sediment-<br>seawater<br>interface | M/N<br>L. Sanzo      | 19-<br>21/09/11         | 9               | 37°12.369N | 15°12.289E          | 22.0               | Benthic chamber<br>(syringe) |           |
|   |                      |                         | 18              | 37°11.294N | 15°12.242E          | 21.0               |                              |           |
|   |                      |                         | 22              | 37°11.406N | 15°12.572E          | 24.0               |                              |           |
|   | M/N<br>L. Sanzo      | 23-<br>26/06/12         | 7               | 37°12.578N | 15°12.583E          | 22.8               |                              |           |
|   |                      |                         | 15              | 37°11.697N | 15°12.917E          | 27.8               |                              |           |
|   |                      |                         | 21              | 37°11.288N | 15°12.459E          | 22.8               |                              |           |

**Table 2:** Total (THg) and dissolved mercury (DHg) concentration measured in the seawater column, inside and outside the bay.

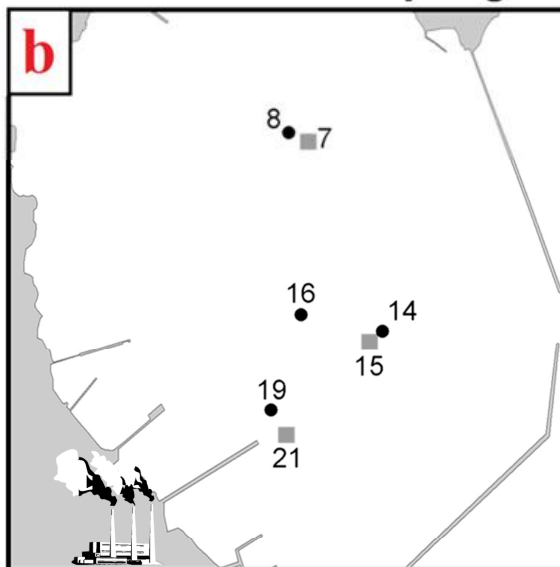
| Sampling period  | Station          | Depth (m) | T (C°) | Salinity (psu) | THg (ngL <sup>-1</sup> ) | DHg (ngL <sup>-1</sup> ) |
|------------------|------------------|-----------|--------|----------------|--------------------------|--------------------------|
| 23-26/05/2011    | Bottom           | 11.2      | 18.0   | 38.0           | 17.8                     |                          |
|                  | <b>1</b> Middle  | 6.20      | 18.4   | 38.0           | 9.17                     |                          |
|                  | Surface          | 1.40      | 20.4   | 38.0           | 9.17                     |                          |
|                  | Bottom           | 10.7      | 18.0   | 38.0           | 17.7                     |                          |
|                  | <b>2</b> Middle  | 6.71      | 18.8   | 38.0           | 14.9                     |                          |
|                  | Surface          | 2.21      | 20.0   | 38.0           | <d.l.                    |                          |
|                  | Bottom           | 8.40      | 18.1   | 38.0           | 30.0                     |                          |
|                  | <b>3</b> Middle  | 4.60      | 19.7   | 38.0           | 12.0                     |                          |
|                  | Surface          | 2.26      | 20.3   | 38.0           | <d.l.                    |                          |
|                  | <b>4</b> Bottom  | 3.12      | 20.2   | 38.0           | 6.30                     |                          |
|                  | Surface          | 0.10      | 20.2   | 38.0           | <d.l.                    |                          |
|                  | Bottom           | 15.9      | 17.7   | 38.0           | 17.7                     |                          |
|                  | <b>5</b> Middle  | 9.20      | 18.5   | 38.0           | 7.10                     |                          |
|                  | Surface          | 1.00      | 19.8   | 38.0           | 9.20                     |                          |
|                  | Bottom           | 13.5      | 18.2   | 38.2           | 20.6                     |                          |
|                  | <b>6</b> Middle  | 6.74      | 19.0   | 37.6           | 3.40                     |                          |
|                  | Surface          | 1.98      | 19.5   | 37.5           | 6.30                     |                          |
|                  | Bottom           | 19.2      | 17.4   | 38.0           | 14.9                     |                          |
|                  | <b>10</b> Middle | 9.50      | 18.8   | 38.0           | 15.9                     |                          |
|                  | Surface          | 1.00      | 20.0   | 39.0           | 4.30                     |                          |
|                  | Bottom           | 18.2      | 17.3   | 38.1           | 23.5                     |                          |
|                  | <b>11</b> Middle | 10.2      | 17.4   | 38.1           | 14.9                     |                          |
|                  | Surface          | 1.42      | 19.3   | 36.7           | 14.9                     |                          |
|                  | Bottom           | 23.4      | 17.0   | 38.1           | 19.3                     |                          |
|                  | <b>12</b> Middle | 13.5      | 17.9   | 37.8           | 3.37                     |                          |
|                  | Surface          | 1.63      | 19.4   | 37.1           | 17.7                     |                          |
|                  | Bottom           | 29.3      | 16.6   | 38.1           | 3.40                     |                          |
|                  | <b>13</b> Middle | 16.9      | 17.4   | 38.1           | 12.7                     |                          |
|                  | Surface          | 2.40      | 19.2   | 38.1           | 17.7                     |                          |
|                  | Bottom           | 21.9      | 17.2   | 38.1           | 127                      |                          |
| <b>17</b> Middle | 11.5             | 18.0      | 38.0   | 129            |                          |                          |
| Surface          | 1.20             | 19.1      | 38.0   | 26.3           |                          |                          |
| Bottom           | 16.5             | 18.3      | 38.0   | 28.2           |                          |                          |
| <b>20</b> Middle | 11.3             | 18.2      | 37.8   | 23.5           |                          |                          |
| Surface          | 0.50             | 19.2      | 38.0   | 20.3           |                          |                          |
| Bottom           | 20.6             | 16.9      | 38.1   | 57.8           |                          |                          |
| <b>23</b> Middle | 11.2             | 18.0      | 38.0   | 20.6           |                          |                          |
| Surface          | 2.40             | 19.0      | 38.0   | 23.4           |                          |                          |
| Bottom           | 16.3             | 17.4      | 38.1   | 23.0           |                          |                          |
| <b>24</b> Middle | 9.40             | 18.7      | 38.0   | 18.7           |                          |                          |
| Surface          | 1.00             | 19.1      | 38.0   | 12.0           |                          |                          |
| Bottom           | 12.7             | 17.7      | 38.1   | 34.9           |                          |                          |
| <b>25</b> Middle | 7.30             | 18.5      | 38.0   | 32.0           |                          |                          |
| Surface          | 1.60             | 19.3      | 38.0   | 22.6           |                          |                          |
| 23-26/06/2012    | Bottom           | 21.0      |        |                | 1.80                     |                          |
|                  | <b>7</b> Middle  | 11.5      |        |                | 9.90                     |                          |
|                  | Surface          | 1.00      |        |                | <d.l.                    |                          |
|                  | Bottom           | 26.0      |        |                | 15.7                     |                          |
|                  | <b>15</b> Middle | 13.5      |        |                | 8.60                     |                          |
|                  | Surface          | 1.00      |        |                | 6.00                     |                          |
|                  | Bottom           | 22.0      |        |                | 18.1                     |                          |
|                  | <b>21</b> Middle | 11.5      |        |                | 14.9                     |                          |
|                  | Surface          | 1.00      |        |                | 1.00                     |                          |

|                     |            |                |                |                |       |       |       |
|---------------------|------------|----------------|----------------|----------------|-------|-------|-------|
| Outside Augusta Bay | 02/02/2012 | <b>26</b>      | <i>Bottom</i>  | 8.00           | 11.1  | 5.55  |       |
|                     |            |                | <i>Surface</i> | 2.00           | 4.55  | <d.l. |       |
|                     |            | <b>27</b>      | <i>Bottom</i>  | 27.0           | 6.10  | 3.55  |       |
|                     |            |                | <i>Middle</i>  | 16.0           | 4.80  | <d.l. |       |
|                     |            | <b>28</b>      | <i>Surface</i> | 2.00           | 4.55  | <d.l. |       |
|                     |            |                | <i>Bottom</i>  | 81.3           | 9.15  | 3.55  |       |
|                     | <b>29</b>  | <i>Middle</i>  | 45.3           | 5.42           | <d.l. |       |       |
|                     |            | <i>Surface</i> | 6.10           | 4.75           | <d.l. |       |       |
|                     |            | <i>Bottom</i>  | 679            | 12.0           | 4.15  |       |       |
|                     |            |                | <b>29</b>      | <i>Middle</i>  | 375   | 6.15  | 5.55  |
|                     |            |                |                | <i>Surface</i> | 20.0  | 2.62  | <d.l. |

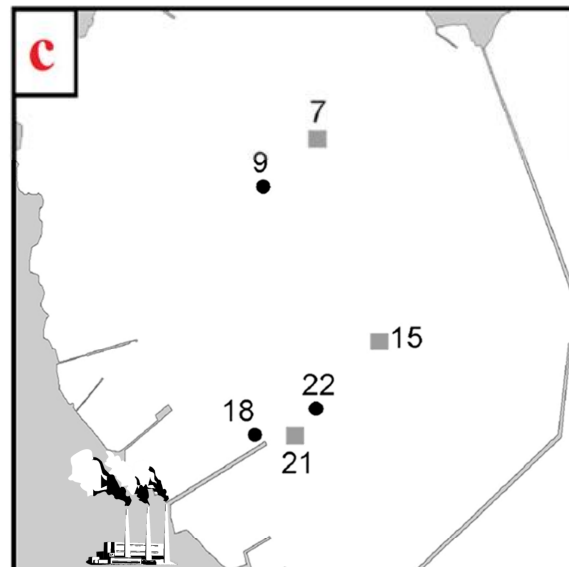
## Seawater sampling



## Sediments sampling

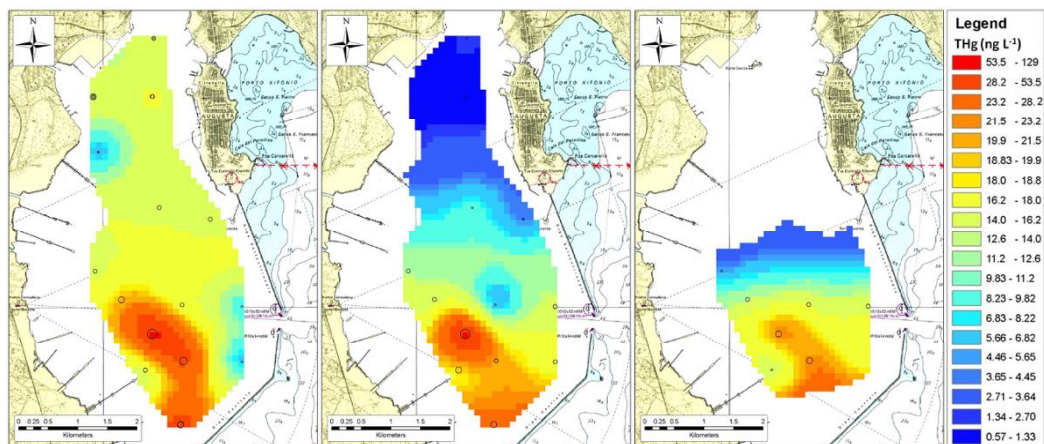


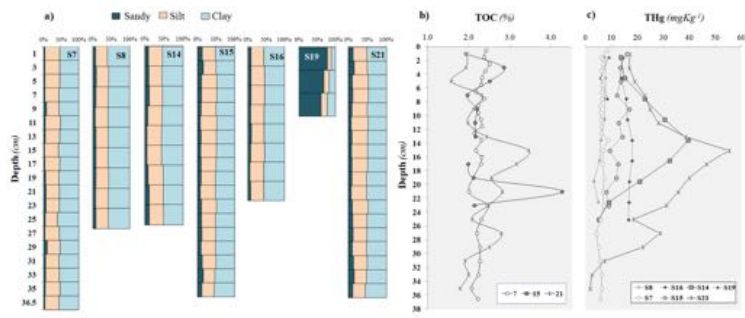
## Benthic chamber

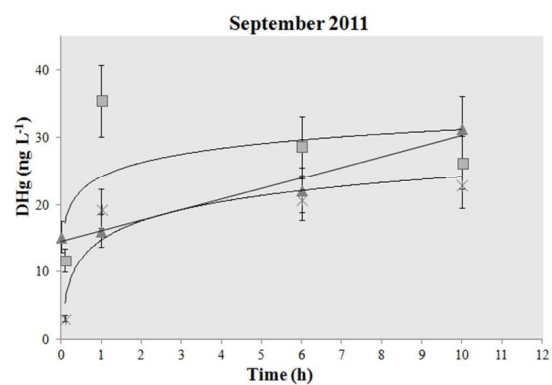


● 2011    ■ 2012

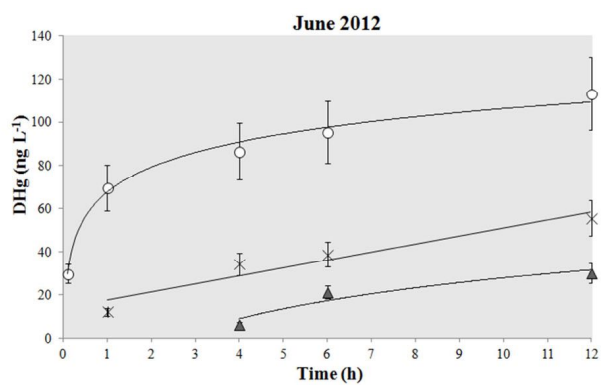








| Station | Regression fit               | $\Phi$<br>( $\mu\text{g m}^{-2} \text{d}^{-1}$ ) |
|---------|------------------------------|--|
| ▲ S9    | $Y=4.1\ln(x)+14.7; R^2=0.88$ | 23   |
| × S18   | $Y=1.6x+14.6; R^2=0.97$      | 56   |
| ■ S22   | $Y=3.0\ln(x)+24.2; R^2=0.40$ | 8.7  |



| Station | Regression fit                | $\Phi$<br>( $\mu\text{g m}^{-2} \text{d}^{-1}$ ) |
|---------|-------------------------------|--|
| ▲ S7    | $Y=20.6\ln(x)-19.7; R^2=0.91$ | 23   |
| ○ S15   | $Y=16.6\ln(x)+67.8; R^2=0.98$ | 92   |
| × S21   | $Y=3.7x+13.8; R^2=0.92$       | 21   |

ACCEPTED MANUSCRIPT